

Live-cell imaging of microRNA expression with post-transcriptional feedback control

Masayuki Sano,¹ Kana Morishita,¹ Satoshi Oikawa,² Takayuki Akimoto,² Kimio Sumaru,¹ and Yoshio Kato³

¹Cellular and Molecular Biotechnology Research Institute, National Institute of Advanced Industrial Science and Technology (AIST), Central 5, 1-1-1 Higashi, Tsukuba, Ibaraki 305-8565, Japan; ²Faculty of Sport Sciences, Waseda University, 2-579-15 Mikajima, Tokorozawa, Saitama 359-1192, Japan; ³Biomedical Research Institute, National Institute of Advanced Industrial Science and Technology (AIST), Central 6, 1-1-1 Higashi, Tsukuba, Ibaraki 305-8566, Japan

MicroRNAs (miRNAs) are small noncoding RNAs that regulate complex gene expression networks in eukaryotic cells. Because of their unique expression patterns, miRNAs are potential molecular markers for specific cell states. Although a system capable of imaging miRNA in living cells is needed to visually detect miRNA expression, very few fluorescence signal-on sensors that respond to expression of target miRNA (miR-ON sensors) are available. Here we report an miR-ON sensor containing a bidirectional promoter-driven Csy4 endoribonuclease and green fluorescent protein, ZsGreen1, for live-cell imaging of miRNAs with post-transcriptional feedback control. Csy4-assisted miR-ON (Csy4-miR-ON) sensors generate negligible background but respond sensitively to target miRNAs, allowing high-contrast fluorescence detection of miRNAs in various human cells. We show that Csy4-miR-ON sensors enabled imaging of various miRNAs, including miR-21, miR-302a, and miR-133, *in vitro* as well as *in vivo*. This robust tool can be used to evaluate miRNA expression in diverse biological and medical applications.

INTRODUCTION

MicroRNAs (miRNAs) are a class of small noncoding RNAs that modulate gene expression.¹ Different types of cells exhibit unique miRNA expression patterns that change dynamically during physical and pathological processes such as differentiation,² tumorigenesis,³ and viral infection.⁴ Dysregulation of miRNA expression is closely associated with onset and progression of a wide spectrum of human diseases; thus, miRNAs are potential therapeutic and diagnostic targets.^{3,5} Strategies targeting miRNAs involved in tumor progression or suppression have been explored extensively for cancer therapy.⁶ In addition, some miRNAs are highly expressed in specific cell types and, in many cases, are directly involved in determining cell fate.^{2,7} Therefore, these miRNAs can serve as unambiguous molecular markers to isolate specific cells from heterogeneous cell populations.^{8,9}

Studies of miRNA expression can reveal the functions of miRNA and be used to evaluate the cell state.^{7,10} Northern blots, microarrays, quantitative reverse-transcriptase PCR, and, most recently, RNA sequencing have been used widely as standard techniques to analyze expression of miRNAs.¹¹ However, these methods are associated with

cell lysis and are thus unsuitable for examining dynamic changes in miRNA expression in living cells. Additionally, the resultant bulk miRNA populations are unlikely to be suitable for single-cell analysis. In contrast, non-invasive techniques based on fluorescence or bioluminescence imaging are highly advantageous for real-time analysis of miRNA expression.¹² Previously, we and others have reported miRNA sensor systems that contain a fluorescent reporter gene harboring multiple complementary sequences against an miRNA of interest in its 3' untranslated region (UTR).^{8,13-16} In these systems, binding of a target miRNA to its complementary sequences causes degradation of reporter-encoded mRNAs,¹ resulting in decreased reporter activity. This type of miRNA sensor (miR-OFF sensor) enables real-time and long-term tracking of miRNA expression in living cells by monitoring the extent of the decrease in fluorescence intensity. miR-OFF sensors have been employed successfully to analyze miRNAs in cultured cells and animals.^{8,17-19}

Despite the significant potency of miR-OFF sensors, it is difficult to discriminate false positives arising for reasons other than miRNA expression because of the mode of miRNA activity detection; i.e., fluorescence disappearance. Importantly, the activity of the promoter that drives the reporter expression varies considerably depending on the cell type, genomic context, and epigenetic control; in some cases, such as long-term cell culture or cell differentiation, a decrease or loss of promoter activity is possible.^{20,21} To decrease the risk of misinterpretation of false positives, an miRNA sensor where fluorescence is generated in response to miRNA expression (miR-ON sensor) is highly desired. Particularly, genetically encoded fluorescence-based miR-ON sensors are advantageous for live-cell imaging of miRNA expression in cultured cells and animals.²²⁻²⁵ Additionally, these miR-ON sensors are potentially applicable for long-term miRNA detection.^{22,26} Thus, miR-ON sensors should be able to confer reliable

Received 12 April 2021; accepted 19 August 2021;
<https://doi.org/10.1016/j.omtn.2021.08.018>.

Correspondence: Masayuki Sano, Cellular and Molecular Biotechnology Research Institute, National Institute of Advanced Industrial Science and Technology (AIST), Central 5, 1-1-1 Higashi, Tsukuba, Ibaraki 305-8565, Japan.
E-mail: m.sano@aist.go.jp

Correspondence: Yoshio Kato, Biomedical Research Institute, National Institute of Advanced Industrial Science and Technology (AIST), Central 6, 1-1-1 Higashi, Tsukuba, Ibaraki 305-8566, Japan.
E-mail: y-kato@aist.go.jp



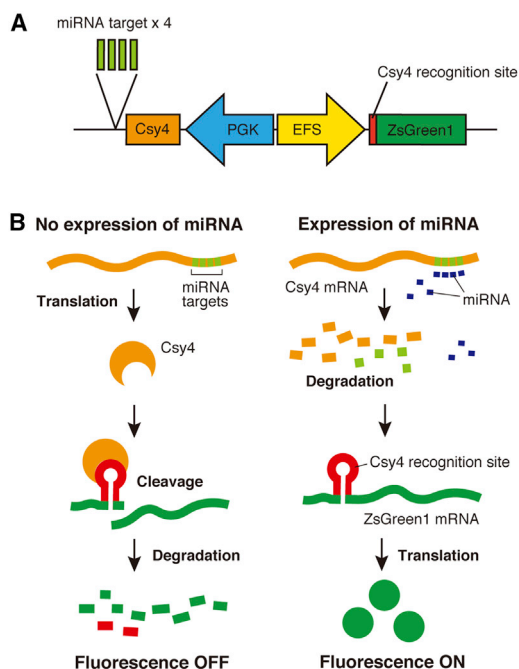


Figure 1. Design of a Csy4-miR-ON sensor

(A) Construction of a Csy4-miR-ON system. The Csy4-miR-ON sensor plasmid contains the bidirectional PGK and EFS promoters to drive expression of Csy4 and ZsGreen1 (ZsG), respectively. Four copies of miRNA target sequence are incorporated into the 3' UTR of Csy4, whereas the Csy4 recognition site is incorporated immediately after the start codon of ZsG. (B) Schematic representation of the feedback mechanism of the Csy4-miR-ON system. Csy4 binds to the Csy4-specific stem loop within the ZsG mRNA and then cleaves it in the absence of the target miRNA, resulting in maintenance of the fluorescence-OFF state. In contrast, Csy4 mRNA is degraded when the miRNA binds to its target sequences. Next, ZsG mRNA is translated, which, in turn, generates a fluorescence signal.

evaluation of miRNA expression in the course of pathogenesis such as tumorigenesis, making it a potential tool for non-invasive diagnosis. Moreover, these sensors could be employed to isolate cells expressing tissue-specific miRNAs after *in vitro* differentiation and cell reprogramming, contributing to preparation of cell sources for cell therapy and regenerative medicine. However, several inherent difficulties, including accurate on/off switching and a gain of an adequate signal/noise ratio, are challenges in the design of an effective miR-ON system capable of sensitively detecting miRNA expression.¹²

In this study, we report an miR-ON system based on post-transcriptional feedback control using miRNA-responsive Csy4. Csy4 is an endoribonuclease responsible for processing precursor transcripts derived from clustered regularly interspaced short palindromic repeats (CRISPRs) in *Pseudomonas aeruginosa*.²⁷ The CRISPR system plays a central role in eliminating invasive parasites in prokaryotes by employing a complex of CRISPR-associated (Cas) protein and CRISPR RNA harboring a sequence complementary to exogenous nucleic acids.²⁸ Csy4 specifically recognizes the 28-nt sequence of the conserved stem loop and then cleaves the 3' end of the stem

base.²⁷ Csy4 has been used in various biological applications, such as RNA-protein binding analysis,²⁹ design of programmable gene networks,^{30,31} and genome editing technology.³² We designed a Csy4-assisted miR-ON (Csy4-miR-ON) sensor containing genes for Csy4 and a reporter fluorescent protein, ZsGreen1 (ZsG), which is driven by a bidirectional promoter. The Csy4-miR-ON sensor can be used for imaging miRNA expression *in vitro* and *in vivo*. Importantly, this sensor produced an inherently low background, allowing high-contrast fluorescence imaging. We provide an invaluable tool for miRNA analysis and for evaluating cell states in diverse biological and medical studies.

RESULTS

Construction of the Csy4-miR-ON sensor

To design the Csy4-miR-ON sensor, we prepared a reporter plasmid containing two mammalian promoters, mouse phosphoglycerate kinase (PGK) and an intron-less form of the human elongation factor 1 α (elongation factor 1 α short [EFS]), that drive expression of Csy4 and ZsG, respectively, in opposite directions (Figure 1A). Both promoters permit efficient transgene expression in a variety of mammalian cells.^{21,33} Because a previous report specified that expression of a reporter gene harboring the Csy4 recognition sequence immediately after the start codon can be degraded efficiently by Csy4 supplied *in trans*,³⁴ the 28-nt stem-loop sequence for Csy4 recognition was cloned immediately after the start codon of ZsG. To modulate Csy4 expression, four copies of the complementary sequence against an miRNA of interest were inserted into the 3' UTR of Csy4 (Figure 1A). In this system, Csy4 is expected to constitutively cleave ZsG mRNA in the absence of target miRNAs, maintaining the fluorescence-OFF state (Figure 1B, left). In contrast, Csy4 mRNA should be cleaved and degraded when target miRNAs bind to their complementary sequences within the Csy4 mRNA. Consequently, ZsG mRNA should be liberated because of Csy4-mediated cleavage, which, in turn, translates into ZsG expression, resulting in maintenance of the fluorescence-ON state (Figure 1B, right).

Imaging of miRNA expression using the Csy4-miR-ON sensors

To investigate the potency of the Csy4-miR-ON sensors for imaging miRNA expression, we constructed a Csy4-miR-ON plasmid containing target sequences of miR-21-5p (21T) as well as a plasmid containing scrambled sequences as a control (CtrlT). Human cervical carcinoma HeLa cells were transfected with either plasmid; expression of ZsG was observed via fluorescence microscopy 1 day after transfection. Based on a dual-luciferase assay using a psiCHECK-2 plasmid harboring a complementary sequence for miR-21-5p at the 3' UTR of the *Renilla* luciferase gene, we confirmed the potent activity of miR-21 in HeLa cells (Figure S1). Robust expression of ZsG was detected in 21T-transfected cells (Figure 2A). In contrast, CtrlT-transfected cells did not exhibit ZsG signals similar to that observed in non-transfected cells under a fluorescence microscope. Flow cytometry indicated that the fluorescence intensity of 21T-transfected cells was considerably higher than that of non-transfected cells. Although CtrlT-transfected cells exhibited somewhat elevated fluorescence intensity compared with non-transfected cells, there was a

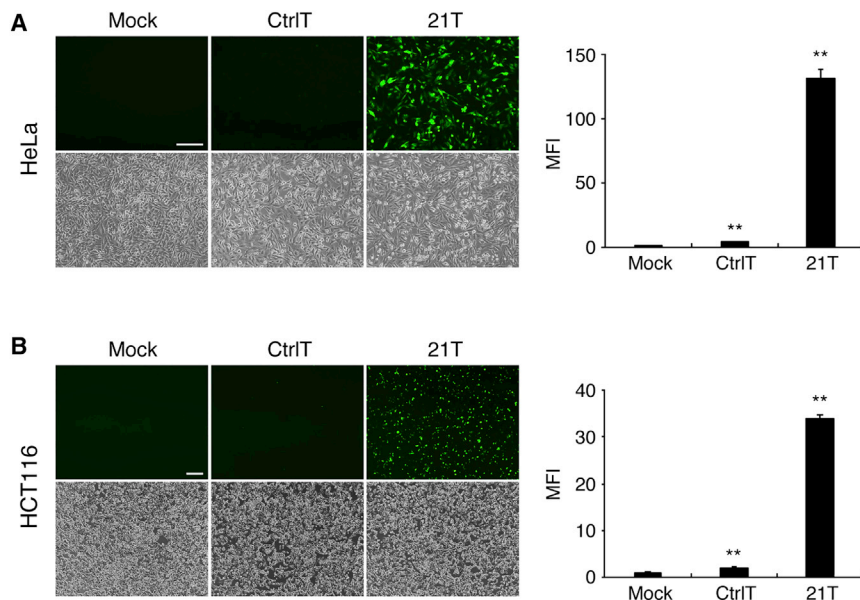


Figure 2. Imaging of miR-21 expression by the Csy4-miR-ON sensor

(A) Imaging of miR-21 expression in HeLa cells. HeLa cells were transfected with the Csy4-miR-ON sensor containing target sequences for miR-21 (21T) or scrambled sequences (CtrlT). One day after transfection, ZsG expression was examined via fluorescence microscopy and flow cytometry. Mean fluorescence intensity (MFI) of non-transfected cells (mock) was set to 1.0, and the relative MFI of Ctrl- and 21T-transfected cells is indicated. Data are presented as the mean \pm SD ($n = 3$). ** $p < 0.001$ versus mock. Pseudo-colored and phase contrast images are shown. (B) Imaging of miR-21 expression in HCT116 cells. Transfection and analyses were performed as described for (A). Data are presented as the mean \pm SD ($n = 3$). ** $p < 0.001$ versus mock. Scale bars, 200 μm .

significant difference between 21T and CtrlT (Figure 2A, right). We also transfected 21T or CtrlT into human colon carcinoma HCT116 cells harboring robust miR-21 activity, as confirmed by a dual-luciferase assay (Figure S1). The sensor plasmid 21T drove robust ZsG expression in HCT116 cells whereas CtrlT did not (Figure 2B). These data indicate that the 21T Csy4-miR-ON sensor could effectively estimate miR-21 expression by detecting ZsG expression.

To confirm the scalability of the Csy4-miR-ON sensors, we prepared the sensor plasmid 122T containing complementary sequences for miR-122-5p and transfected it into human hepatocellular carcinoma HuH-7 cells, which express high levels of miR-122.³⁵ Fluorescence microscopy and flow cytometry indicated that 122T resulted in a marked increase in ZsG signal compared with that observed in non-transfected and CtrlT-transfected cells (Figure S2), suggesting that the Csy4-miR-ON sensors can be used to effectively image endogenous miRNA expression.

Sensitivity of the Csy4-miR-ON sensors for detecting miRNA activity

Next we examined the sensitivity of the Csy4-miR-ON sensors using an exogenously supplied miRNA inhibitor and mimic oligonucleotides. First, to inhibit the activity of endogenous miR-21, HeLa cells were co-transfected with the 21T sensor and an miR-21 inhibitor; ZsG expression was then examined via fluorescence microscopy. We observed no apparent ZsG signal when the miR-21 inhibitor was co-transfected with 21T, whereas the Ctrl inhibitor drove robust expression of ZsG in 21T-transfected cells (Figure 3A, left). Flow cytometry indicated that the miR-21 inhibitor markedly decreased ZsG expression compared with the Ctrl inhibitor (Figure 3A, right). These data suggest that the 21T sensor responds sensitively to endogenous miR-21 activity.

We also generated a sensor plasmid containing complementary sequences for miR-302a-3p (302aT) and co-transfected this plasmid along with the miR-302a mimic into HeLa cells. Because miR-302a is expressed specifically in pluripotent stem cells,³⁶ such as embryonic stem cells (ESCs) and induced pluripotent stem cells (iPSCs), HeLa cells do not exhibit significant expression of miR-302a.⁷ Transfection with the miR-302a mimic markedly increased the ZsG signal (compared with that observed with the Ctrl mimic; Figure 3B, left). These data correlated well with those obtained via flow cytometry, indicating the high sensitivity of the 302aT sensor to the exogenously supplied miR-302a mimic (Figure 3B, right). We found that the fluorescence intensity of Ctrl mimic-transfected cells was slightly higher than that of non-transfected cells. This suggests that the 302aT sensor may respond to endogenous miRNAs other than miR-302a in HeLa cells. Previous studies demonstrated that miRNAs can promote translational repression and/or mRNA degradation by binding to target sequences with partial complementarity.^{1,37} Thus, seed sequence positioning at bases 2–8 from the 5' end of miRNA is essential for miRNA function.³⁸ Therefore, the 302aT sensor may respond to some miRNAs, such as miR-17 and/or miR-20a, which contain a seed sequence identical to that of miR-302a-3p.³⁹

Improvement in the sensitivity of the Csy4-miR-ON sensors

Although Csy4-miR-ON sensors gave rise to adequate levels of ZsG signal in HeLa and HCT116 cells, the low transfection efficiency of the plasmid may result in decreased fluorescence intensity. Thus, it may be difficult to gain a sufficient signal/noise ratio in hard-to-transfect cells such as primary culture cells and *in vivo* tissue cells. To improve the sensitivity of Csy4-miR-ON sensors, we designed a reporter plasmid containing a single copy of the miRNA target sequence at the 5' UTR of Csy4 in addition to four copies of the target sequence at its 3' UTR (Figure 4A). Because a single complementary sequence for a target miRNA at the 5' UTR of the reporter gene has been shown to be susceptible to miRNA-mediated inhibition,⁹ we predicted that incorporation of multiple miRNA

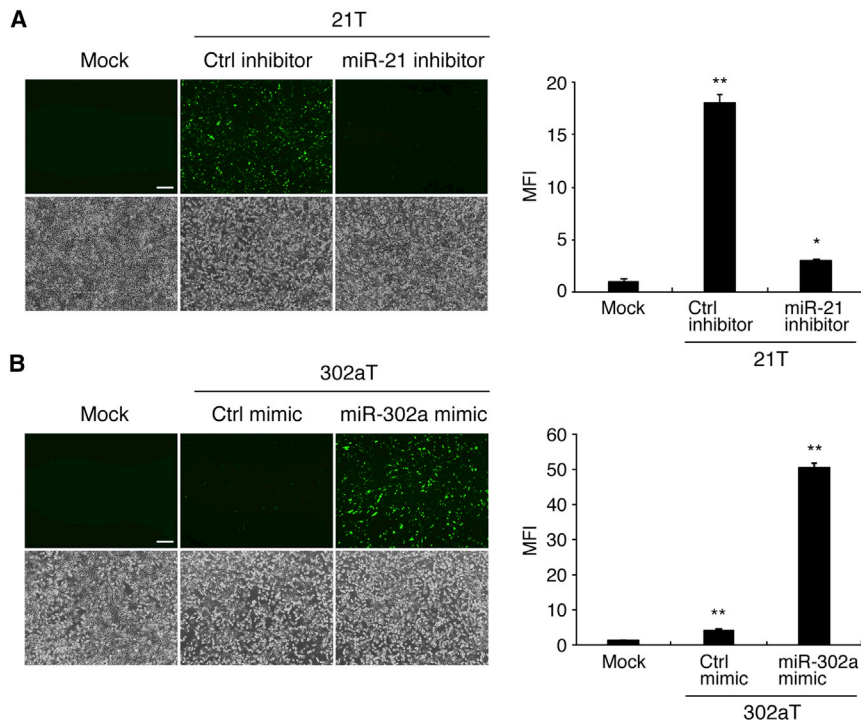


Figure 3. Sensitive response of the Csy4-miR-ON sensors to miRNA activity

(A) Evaluation of the Csy4-miR-ON sensor using an miRNA inhibitor. HeLa cells were co-transfected with the 21T sensor and miR-21 inhibitor, and ZsG expression was examined by fluorescence microscopy and flow cytometry 1 day after transfection. As a control, the control inhibitor (Ctrl inhibitor) was used rather than the miR-21 inhibitor. The MFI of non-transfected cells (mock) was set to 1.0, and the relative MFI of Ctrl inhibitor- and miR-21 inhibitor-transfected cells is indicated. Data are presented as the mean \pm SD ($n = 3$). * $p < 0.005$, ** $p < 0.001$ versus mock. Pseudo-colored and phase contrast images are shown; scale bar, 200 μ m. (B) Evaluation of the Csy4-miR-ON sensor using an miRNA mimic. HeLa cells were co-transfected with the 302aT sensor and the miR-302a mimic, and analyses were performed as described for (A). As a control, the control mimic (Ctrl mimic) was used rather than the miR-302a mimic. The MFI of mock cells was set to 1.0, and the relative MFI of Ctrl mimic- and miR-302a mimic-transfected cells is indicated. Values and scale bar are the same as those described for (A). ** $p < 0.001$ versus mock.

target sites at the 5' and 3' UTRs of *Csy4* could enhance the sensitivity of Csy4-miR-ON sensors for target miRNAs. To evaluate the efficacy of this modification, we constructed a sensor plasmid containing complementary sequences for miR-302a-3p at the 5' and 3' UTRs of *Csy4* (302aTT') and a plasmid containing scrambled sequences at the same position as the control (CtrlTT'). Embryonic carcinoma NTERA-2 (NT-2) cells were transfected with CtrlT, CtrlTT', 302aT, or 302aTT', and ZsG signals were subsequently examined via fluorescence microscopy. NT-2 cells have been shown to express ESC-specific miRNAs, including miR-302a.⁷ Although 302aT- and 302aTT'-transfected cells harbored positive ZsG signals relative to CtrlT- and CtrlTT'-transfected cells, 302aTT' conferred robust signal intensity compared with 302aT (Figure 4B). Flow cytometry indicated that the fluorescence intensities of 302aT- and 302aTT'-transfected cells were 9- and 37-fold higher than that of non-transfected cells, respectively (Figure 4C). These data suggest that incorporation of multiple target sequences at the 5' and 3' UTRs remarkably improved the sensitivity of the Csy4-miR-ON sensor.

Csy4-miR-ON sensors enable discrimination of miRNA expression in different cells

We evaluated the potency of Csy4-miR-ON sensors in human iPSCs (hiPSCs) and normal human dermal fibroblasts (NHDFs). Because these cells exhibit a striking inverse correlation between the expression of miR-302a and *Let-7a*,^{16,40} we examined whether Csy4-miR-ON sensors could properly discriminate the expression of these miRNAs. We prepared a sensor plasmid containing complementary sequences for *Let-7a-5p* at the 5' and 3' UTRs of *Csy4* (*Let7aTT'*) and transfected 302aTT' or *Let7aTT'* into hiPSCs and NHDFs. As

expected, 302aTT' gave rise to a ZsG signal in hiPSCs but not in NHDFs, whereas *Let7aTT'* was present only in NHDFs (Figure 5A). The control CtrlTT' sensor showed no significant positive signals in either cell line. These data suggest that Csy4-miR-ON sensors enable a clear distinction of miRNA expression in different cells.

An advantage of miR-ON sensors is that they can be readily employed for multi-color imaging. For this, hiPSCs were transfected with CtrlTT' or 302aTT', and expression of the ESC-specific marker protein NANOG was examined via immunofluorescence staining in Csy4-miR-ON sensor-transfected cells. The expression of ZsG and NANOG was detected simultaneously in 302aTT'-transfected hiPSCs, suggesting that Csy4-miR-ON sensors can be used for multi-color imaging of miRNA and protein expression (Figure 5B).

Detection of a muscle-specific miRNA via the Csy4-miR-ON sensor

We have previously reported that the miR-OFF sensor can monitor muscle-specific expression of miR-133 during differentiation of mouse myoblast C2C12 cells into myotubes.¹³ The expression of miR-133 was apparent in differentiated myotubes but not in myoblasts.¹³ To examine the miR-133 expression, we constructed a Csy4-miR-ON sensor plasmid containing complementary sequences for miR-133-3p at the 5' and 3' UTRs of *Csy4* (133TT'). C2C12 cells were transfected with 133TT' or the control sensor CtrlTT' and then cultured in differentiation medium for 6 days. Although ZsG expression was not significant in 133TT'-transfected C2C12 cells, its expression was markedly upregulated in myotubes (Figure 6A). Notably, the ZsG signal was negative in myotubes that had been transfected with

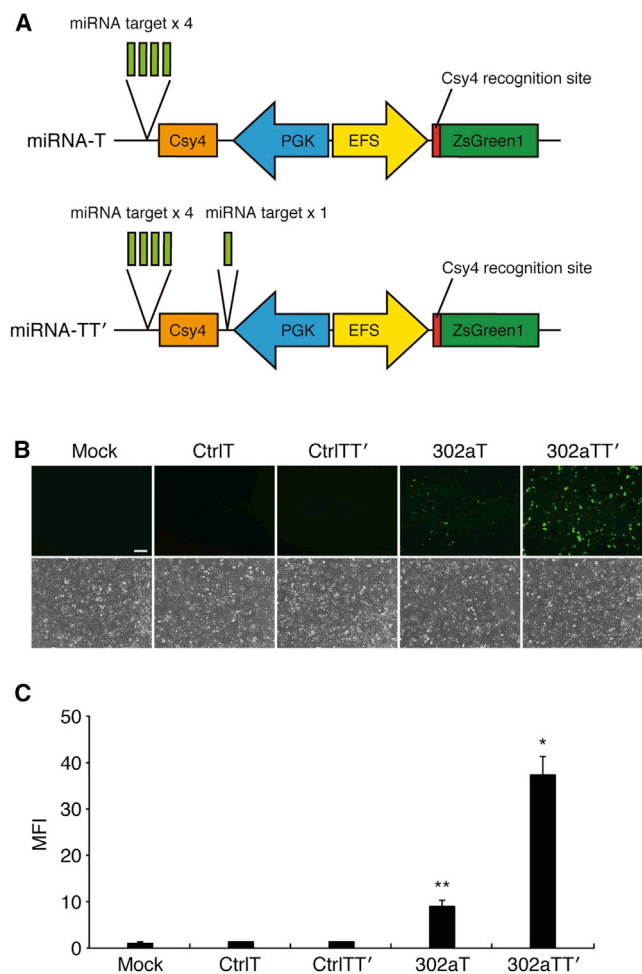


Figure 4. Improved sensitivity of the Csy4-miR-ON sensors

(A) Construction of the Csy4-miR-ON sensor with modifications. The modified Csy4-miR-ON sensor (miRNA-TT') contains four copies of miRNA target sequences at the 3' UTR as well as a single copy of the miRNA target sequence at the 5' UTR of Csy4, whereas the original Csy4-miR-ON sensor (miRNA-T) contains four copies of miRNA target sequences at the 3' UTR of the Csy4 gene. (B) Imaging of miR-302a expression by the modified Csy4-miR-ON sensor. NT-2 cells were transfected with CtrlIT, CtrlTT', 302aT, or 302aTT', and ZsG expression was examined via fluorescence microscopy 1 day after transfection. CtrlIT and 302aT were constructed using the miRNA-T backbone, whereas CtrlTT' and 302aTT' were constructed using miRNA-TT'. Pseudo-colored and phase contrast images are shown; scale bar, 200 μ m. (C) Quantitative evaluation of the modified Csy4-miR-ON sensor. Sensor plasmid-transfected cells were analyzed via flow cytometry. The MFI of non-transfected cells (mock) was set to 1.0, and the relative MFI of each sensor-transfected cell is indicated. Data are presented as the mean \pm SD (n = 3). *p < 0.005, **p < 0.001 versus mock.

CtrlTT'. These data indicate that 133TT' responded sensitively to miR-133 expression during myogenesis.

Finally, we attempted *in vivo* imaging of miRNA expression using Csy4-miR-ON sensors. Either CtrlTT' or 133TT' was injected into the *tibialis anterior* (TA) muscles in mice, and TA muscles were har-

vested 5 days after injection. Confocal laser microscopy indicated that 133TT' gave rise to a robust ZsG signal whereas CtrlTT' did not (Figure 6B). Importantly, CtrlTT' exhibited negligible background in muscle tissue. These data suggest that Csy4-miR-ON sensors allow high-sensitivity and high-contrast fluorescence imaging in response to miRNA activity *in vivo*.

DISCUSSION

Because of their cell-dependent expression profiles, miRNAs are potential molecular targets and markers for diverse biological and medical research, including cancer and stem cell research. miR-21, miR-155, and the miR-17-92 cluster are upregulated in many cancer cells, whereas the Let-7 and miR-34 families are often downregulated.³ Thus, these miRNAs can be exploited as biomarkers for early diagnosis and prognosis. Additionally, tissue-specific miRNAs such as miR-302a, miR-122, and miR-208a can be used to specifically identify and isolate iPSCs, hepatocytes, and cardiomyocytes, respectively.^{8,9} To examine miRNA expression and evaluate specific cell states, fluorescence-based miRNA sensors are advantageous because of their simple, sensitive, and non-invasive properties.

Fluorescence signal-on sensors would be highly beneficial for evaluating miRNA expression, but very few miR-ON systems are currently available. A tetracycline repressor (rTA)-fused Krüppel-associated box (KRAB) was exploited to design the miR-ON system.²² In this system, the GFP signal is activated in response to miRNA-mediated rTA-KRAB inhibition, whereas rTA-KRAB inhibited GFP expression in the absence of the target miRNA. Additionally, the Cumate gene switch-inducible system was cloned into the miR-ON system, resulting in generation of bioluminescent signals depending on miRNA activity.²⁶ Apart from transcriptional control, translational control using the translational repressor L7Ae has also been employed in the design of the miR-ON system.²⁴ These three systems utilize a similar concept in that a target miRNA inhibits expression of repressor proteins by binding to the 3' UTR of the repressor-encoded mRNA, followed by "switching on" reporter expression. Although we designed the Csy4-miR-ON system using a similar concept, our system is clearly distinct from existing systems because the Csy4-miR-ON sensor exploits post-transcriptional feedback control with Csy4 and miRNAs. Recently, a light-up RNA aptamer has been shown to allow live-cell imaging of miRNA expression.²³ Although this strategy permits direct detection of miRNA expression via interactions of the aptamer with target miRNAs, colocalization of fluorophore sulforhodamine quencher conjugates with aptamers is required to obtain fluorescence. Additionally, nuclease-deficient Cas9-mediated transcriptional activation has been used to design an miR-ON system.²⁵ Although this system could respond sensitively to miRNA activity, co-transduction of multiple gene expression units is required for imaging. Currently, effective genetically encoded miR-ON sensors remain limited in terms of accessibility, likely because of inherent difficulties such as the high background and low signal/noise ratio, particularly *in vivo*.¹² Our Csy4-miR-ON sensors exhibited low levels of inherent background but high fluorescence signals in response to the target miRNA in transfected culture cells and even in animal

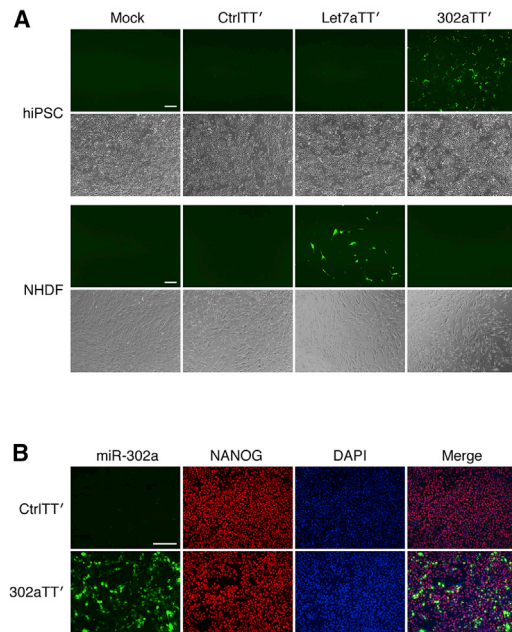


Figure 5. Capability of Csy4-miR-ON sensors for imaging analyses

(A) Imaging of miRNA expression in hiPSCs and NHDFs. hiPSCs and NHDFs were transfected with CtrlTT', Let7aTT', or 302aTT', and ZsG expression was examined via fluorescence microscopy 1 day after transfection. Pseudo-colored and phase contrast images are shown; scale bars, 200 μ m. (B) Co-imaging of miR-302a and NANOG expression. hiPSCs were transfected with CtrlTT' or 302aTT', and NANOG expression was analyzed by immunofluorescence staining. Nuclei were counterstained with DAPI. Pseudo-colored images are shown; scale bars, 200 μ m.

tissues. Moreover, the Csy4-miR-ON sensor was able to track expression of the muscle-specific miR-133 for a sufficient period during myogenesis. Therefore, this system should contribute to identification of target cells harboring miRNAs as markers and specific isolation of these cells from heterogeneous cell populations. These strategies are particularly important for obtaining specific cells in *in vitro* differentiation and cell reprogramming methodologies.⁹

The miR-ON sensor system can be applied not only for endogenous miRNAs but also for exogenous miRNAs. Circulating miRNAs have received much attention as diagnostic markers, and these miRNAs released from specific tissues can be sampled as biofluids from blood or urine. Extracellular miRNAs enveloped in small vesicles, also known as exosomes, are sometimes taken up into other tissues.^{41,42} Additionally, recent studies revealed that plant and viral miRNAs taken up by animals via food play a role in regulating host transcriptional networks.^{43,44} The Csy4-miR-ON sensor may be applied as an evaluation method for the function of circulating miRNAs as well as *trans*-supplied miRNAs in cross-kingdom interaction. Furthermore, a recent study suggested that the new coronavirus severe acute respiratory syndrome coronavirus 2 (SARS-CoV-2) encodes miRNAs in their genomes to suppress a variety of host anti-viral genes.⁴⁵ Although PCR is often used to detect viral RNAs, it only evaluates the amounts of RNA molecules regardless of whether the viruses

are infectious. In our previous study, we succeeded in quantitatively monitoring adenovirus-encoded miR-VAI using the miR-OFF sensor.¹⁴ Our Csy4-miR-ON system may be a useful tool for evaluating the existence of infectious viruses, including SARS-CoV-2, through detection of viral miRNAs.

To design Csy4-miR-ON sensors, we employed bidirectional PGK and EFS promoters to drive expression of Csy4 and ZsG, respectively. Our data suggest that combination of these promoters can properly control the levels of Csy4 and ZsG expression in various cultured cells and in mice. Although we demonstrated the significant potency of Csy4-miR-ON sensors in transient assays, the system may be used for long-term evaluation of miRNA expression during changes in the cell state, such as tumorigenesis, differentiation, and cell reprogramming. We reported previously that the retrovirus-, lentivirus-, and Sendai virus-based miR-OFF sensors are able to monitor miRNA expression in cells stably transduced with these sensors.^{13,14,16} The Csy4-miR-ON system should readily transfer to these vector backbones for long-term imaging of miRNA expression. Unlike the present Csy4-miR-ON system, the previous miR-OFF sensors contained green and red fluorescent proteins (GFP and RFP, respectively) for dual-color imaging.^{13,14,16} In this system, GFP and RFP were used as the reporter and internal reference, respectively. The advantage of the dual-color system is that detection of RFP can readily discriminate cells with fluorescence quenching from non-transduced cells, enabling reliable interpretation. In contrast to the miR-OFF sensors, the miR-ON sensors give rise to fluorescence signals responding to target miRNA expression, conferring a low possibility of generating false positives. However, dual-color imaging is beneficial for establishing a more reliable assay system. Thus, further refinement of the Csy4-miR-ON system will improve the longevity and reliability of miRNA detection.

Multi-color imaging of protein expression via fluorescence immunostaining is a standard technique for evaluating patterns of protein expression as well as identifying the cell state. Because of the unique expression profiles of miRNAs in specific cell types, co-imaging of proteins with miRNAs should be beneficial for stringently evaluating the cell state. We showed that Csy4-miR-ON sensors can be exploited for co-imaging of miR-302a and NANOG proteins in hiPSCs. So far, co-imaging of miRNAs with proteins has mostly relied on an *in situ* hybridization technique.¹¹ However, this technique requires fixation of cells before imaging. Although we performed fluorescence immunostaining with fixed hiPSCs, Csy4-miR-ON sensors may allow simultaneous detection of miRNAs and proteins in combination with cell-permeable fluorescent dyes in living cells.⁴⁶ Thus, Csy4-miR-ON sensors may support live-cell imaging of miRNAs and proteins to identify cell states and examine the expression networks between proteins and miRNAs.

In summary, our findings demonstrate that Csy4-miR-ON sensors enable live-cell imaging of miRNA expression with post-transcriptional feedback control. This system gives rise to high-contrast fluorescence signals responding to target miRNA expression, suggesting

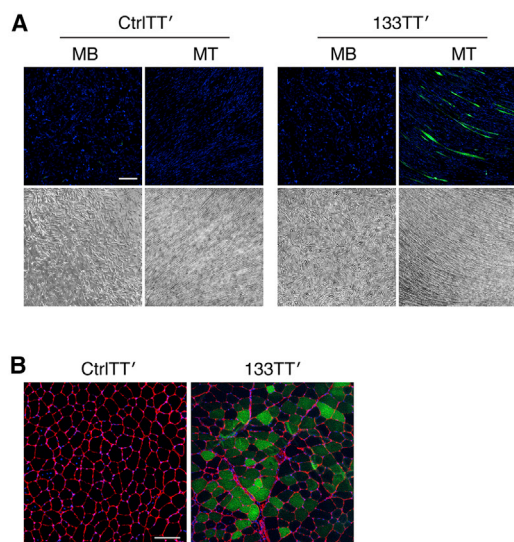


Figure 6. Imaging of a muscle-specific miRNA with the Csy4-miR-ON sensor

(A) Live-cell imaging of miR-133 expression. C2C12 cells were transfected with CtrlTT' or 133TT', and miR-133 expression was monitored during myogenesis. Nuclei were counterstained with Hoechst 33342. Pseudo-colored images are shown; scale bar, 200 μ m. MB, myoblasts; MT, myotubes. (B) Representative images of muscle section with Csy4-miR-ON sensors. Electric pulse-mediated gene transfer was performed to express CtrlTT' or 133TT' in the *tibialis anterior* (TA) muscle of C57Bl6 wild-type (WT) mice. Five days after gene transfer, the mice were sacrificed to collect TA muscles. Cross-section of TA were stained with Hoechst 33342 (blue, nucleus) and anti-laminin antibody (red, sarcolemma). Scale bar, 100 μ m.

that it is a powerful tool for evaluating miRNA expression *in vitro* and *in vivo*. Regulatory switch systems have been extensively studied to control gene expression through transcription, translation, and post-transcriptional regulation.⁴⁷ Interestingly, miRNA-mediated switch systems can be exploited for inducible CRISPR-Cas9 activation^{35,48} and selective killing of cancer cells.²⁴ Because of the inherent high signal/noise ratio, our system may also be applied for designing an effective switch system. Further efforts will expand the potential of the Csy4-miR-ON system to contribute to a broad range of biological and medical studies.

MATERIALS AND METHODS

Plasmid construction

The DNA fragment containing the EFS promoter was amplified by PCR using pTracer-EF/Bsd (Invitrogen, Carlsbad, CA, USA) with the primers 5'-AAAAAGCGCCGCGGCTCCGGTGCCCCG TCA-3' and 5'-GGTGGCTAGCTCACGACACCTGTGTTCTGGC GG-3' and inserted into the *NotI* and *NheI* sites of pLV.SGb.PtR¹⁴ to yield pLV.SGb.FtR. The DNA fragment containing the PGK promoter was prepared as described previously¹⁴ and inserted into the *NotI* and *XbaI* sites of pLV.SGb.FtR to yield pLV.PGb.FtR. To prepare the cDNA encoding ZsG with the Csy4 recognition sequence (Csy4RS-ZsG), the DNA fragment was amplified by PCR using the

pmR-ZsGreen1 (Clontech Laboratories, Mountain View, CA, USA) as a template with the primers 5'-ATGGCCAGTCCAAGC ACGGC-3' and 5'-GGTGGCGACCGGTAGCGCTAG-3'. The hybridized sense (5'-CTACCGGTCGCCACCATGAGTTCAGTGC CGTATAGGCAGCTAAGAAATATGGCCAGTCCAAG-3') and antisense (5'-CTTGGACTGGGCCATATTTCTTAGCTGCCTATA CGGCAGTGAACCTCATGGTGGCGACCGGTAG-3') strands were inserted into the PCR fragment using the In-Fusion HD Cloning Kit (Clontech). cDNA encoding Csy4RS-ZsG was amplified by PCR using the obtained plasmid as a template with primers 5'-CTCAGC TAGCCACCATGAGTTCAGTGCCTATAGG-3' and 5'-AATCC TCGAGCTAGTTTCCGGAGGGCAAGGC-3'. To prepare cDNA encoding Csy4, human-codon-optimized Csy4 was synthesized by GenScript (Piscataway, NJ, USA). The cDNAs encoding Csy4RS-ZsG and Csy4 were inserted into the *NheI/XhoI* and *EcoRI/XbaI* sites of pLV.PGb.FtR, respectively, to yield pLV.PC.FCRS-Z. To construct the Csy4-miR-ON sensor (pLV.PCt4.FCRS-Z), DNA fragments containing four copies of the complementary sequence for the target miRNA were prepared as described previously^{16,49} and inserted into the *EcoRI* site of pLV.PC.FCRS-Z. To construct the modified Csy4-miR-ON sensor (pLV.PCt'1t4.FCRS-Z), hybridized sense (miR-302a, 5'-CTAGTCACCAAAACATGGAAGCACTTA-3'; Let-7a, 5'-CTAGAACTATACAACCTACTACCTCA-3'; miR-133, 5'-CTAGCAGCTGGTTGAAGGGGACCAAAA-3'; scramble, 5'-CTAG GTGCTCTAACCTTCTCGTAAGA-3') and antisense (miR-302a, 5'-CTAGTAAGTGCTTCCATGTTTTGGTGA-3'; Let-7a, 5'-CTAG TGAGGTAGTAGTTGTATAGTT-3'; miR-133, 5'-CTAGTTTG GTCCCCTTCAACCAGCTG-3'; scramble, 5'-CTAGTCTTACGA GAAGGTTAGAGCAC-3') strands were inserted into the *XbaI* site of pLV.PCt4.FCRS-Z. The scrambled sequence was predicted using the siRNA Wizard v.3.1 software (InvivoGen, San Diego, CA, USA). For the dual-luciferase assay, the reporter plasmids psi-miR-21T and psi-miR-scr were constructed using psiCEHCK-2 (Promega, Madison, WI, USA), as described previously.⁴⁹

Cell culture and transfection

HeLa, HCT116, HuH-7, NT-2, and NHDFs (Kurabo, Osaka, Japan) were cultured in Dulbecco's modified Eagle's medium (DMEM; Sigma-Aldrich, St. Louis, MO, USA) supplemented with 10% fetal bovine serum (FBS; HyClone Laboratories, Logan, UT, USA) and penicillin-streptomycin (Wako Pure Chemicals Industries, Osaka, Japan). hiPSCs were cultured in AK02N (Ajinomoto, Tokyo, Japan) on a plate coated with iMatrix-511 (Nippi, Tokyo, Japan). HeLa, HCT116, and HuH-7 cells were grown to ~70%–80% confluence in 12-well plates and transfected with 1 μ g of Csy4-miR-ON plasmid using Lipofectamine 2000 transfection reagent (Thermo Fisher Scientific, Waltham, MA, USA). NT-2 and hiPSCs were grown to ~70%–80% in 12-well plates and transfected with 1 μ g of Csy4-miR-ON plasmid using Lipofectamine Stem transfection reagent (Thermo Fisher Scientific). NHDFs were grown to ~80%–90% confluence in a 12-well plate and transfected with 1 μ g of Csy4-miR-ON plasmid using Lipofectamine LTX transfection reagent (Thermo Fisher Scientific). C2C12 cells were grown to 70% confluence in a 6-well plate and transfected with 5 μ g of Csy4-miR-ON plasmid using Lipofectamine

2000. For induction of myogenesis, DMEM with 10% FBS was replaced with differentiation medium comprising DMEM with 2% horse serum 2 days after transfection. For transfection of miRNA inhibitors, HeLa cells were grown to ~90% confluence in a 12-well plate and co-transfected with 1 μ g of Csy4-miR-ON 21T plasmid and 20 nM of mirVana miR-21-5p or control inhibitor (Thermo Fisher Scientific) using Lipofectamine 2000. For transfection of miRNA mimics, HeLa cells were grown to ~80% confluence in a 12-well plate and co-transfected with 1 μ g of Csy4-miR-ON 302aT plasmid and 10 nM of mirVana miR-302a-3p or control mimic (Thermo Fisher Scientific) using Lipofectamine 2000.

Fluorescence microscopy and image acquisition

ZsG expression was detected under a fluorescence microscope (Axio Observer.A1, Zeiss, Oberkochen, Germany or C1 microscope system, Nikon, Tokyo, Japan) using a customized filter. Fluorescence was analyzed using iVision-Mac software (Solution Systems, Funabashi, Japan) or NIS-elements software (Nikon). Co-imaging of fluorescence for ZsG, Alexa Fluor 555 (Thermo Fisher Scientific), 4',6-diamidino-2-phenylindole (DAPI), and Hoechst 33342 was performed using an Axio Observer or C1 microscope system.

Flow cytometry analysis

Cells were seeded into a 12-well plate and transfected with 1 μ g of Csy4-miR-ON sensor plasmid using a transfection reagent appropriate for the cell type. The following day, the cells were harvested, and flow cytometry was performed using a Gallios flow cytometer (Beckman Coulter, Brea, CA, USA). The mean fluorescence intensity (MFI) was calculated using Kaluza software (Beckman Coulter).

Immunofluorescence staining

Cells were fixed with 3.7% formaldehyde in PBS and permeabilized with 0.1% Triton X-100 in PBS. The cells were then incubated with an anti-NANOG antibody (1:20; R&D Systems, Minneapolis, MN, USA), followed by staining with a secondary antibody conjugated to Alexa Fluor 555 (1:500). Nuclei were counterstained with DAPI using VECTASHIELD mounting medium with DAPI (Vector Laboratories, Burlingame, CA, USA).

Luciferase assay

To determine the luciferase activity of psi-miR-21T and psi-miR-scr, HeLa and HCT116 cells were grown to ~60% confluence in 48-well plates and transfected with 25 ng of the plasmid using Lipofectamine 2000 reagent. 24 h later, the activity of firefly and *Renilla* luciferase was analyzed using the Dual-Luciferase Reporter Assay System (Promega).

Electric pulse-mediated gene transfer

Electric pulse-mediated gene transfer was performed as described previously.⁵⁰ Briefly, both TA muscles were injected with 20 μ g of plasmid DNA under anesthesia (50 mg/kg intraperitoneal [i.p.] sodium pentobarbital). Within 1 min after injection, an electrical field was delivered to the injected TA muscle using a SEN-3401 electric stimulator (Nihon Kohden, Tokyo, Japan) through a Model 532

two-needle array (BTX Instrument Division Harvard Apparatus, Holliston, MA, USA). Eight pulses with a duration of 100 ms, frequency of 1 Hz, and amplitude of 100 V (200 V/cm) were delivered by placing the needle arrays on the medial and lateral sides of the TA muscle so that the electrical field was perpendicular to the long axis of the myofibers. The mice were allowed to recover for 5 days before collecting the TA muscle. The procedures of animal experiments were approved by the Animal Care and Use Committees of Waseda University, Japan (numbers: 2019-A108, 2020-A012) and performed in accordance with the institutional and national guidelines.

Immunohistochemistry

Optimal cutting temperature compound-embedded cross-sections of mouse skeletal muscle were used for immunostaining.⁵⁰ A rabbit anti-laminin antibody (10765, Cappel) with an Alexa 549-conjugated secondary antibody (Jackson ImmunoResearch Laboratories, West Grove, PA, USA) was used to identify the muscle fiber shape. Cross-sections were fixed in PBS with 4% paraformaldehyde, permeabilized in PBS with 0.3% Triton X-100, incubated with primary antibody overnight, and then incubated with secondary antibody and Hoechst 33342 (1:10,000) for 1 h at room temperature. Finally, coverslips were mounted in VECTASHIELD mounting medium (Vector Laboratories). Cross-sections were photographed using a C2 confocal microscope system (Nikon).

Statistical analysis

The data are presented as the mean \pm SD. Statistical analyses were performed using a two-tailed Student's t test.

SUPPLEMENTAL INFORMATION

Supplemental information can be found online at <https://doi.org/10.1016/j.omtn.2021.08.018>.

ACKNOWLEDGMENTS

This work was supported in part by JSPS KAKENHI (grants 19K06501 to M.S., 20K20620 to T.A., and 19H02578 to K.S.).

AUTHOR CONTRIBUTIONS

M.S. and Y.K. conceived the study. M.S., T.A., and Y.K. designed the study. M.S., K.M., S.O., and Y.K. performed the experiments. M.S., K.M., S.O., and K.S. analyzed the data. M.S. and Y.K. wrote the manuscript. All authors reviewed and edited the manuscript.

DECLARATION OF INTERESTS

The authors declare no competing interests.

REFERENCES

- Bartel, D.P. (2004). MicroRNAs: genomics, biogenesis, mechanism, and function. *Cell* 116, 281–297.
- Sun, K., and Lai, E.C. (2013). Adult-specific functions of animal microRNAs. *Nat. Rev. Genet.* 14, 535–548.
- Lujambio, A., and Lowe, S.W. (2012). The microcosmos of cancer. *Nature* 482, 347–355.

4. Trobaugh, D.W., and Klimstra, W.B. (2017). MicroRNA regulation of RNA virus replication and pathogenesis. *Trends Mol. Med.* 23, 80–93.
5. Wang, M., Yu, F., Ding, H., Wang, Y., Li, P., and Wang, K. (2019). Emerging function and clinical values of exosomal microRNAs in cancer. *Mol. Ther. Nucleic Acids* 16, 791–804.
6. Hayes, J., Peruzzi, P.P., and Lawler, S. (2014). MicroRNAs in cancer: biomarkers, functions and therapy. *Trends Mol. Med.* 20, 460–469.
7. Landgraf, P., Rusu, M., Sheridan, R., Sewer, A., Iovino, N., Aravin, A., Pfeffer, S., Rice, A., Kamphorst, A.O., Landthaler, M., et al. (2007). A mammalian microRNA expression atlas based on small RNA library sequencing. *Cell* 129, 1401–1414.
8. Brown, B.D., Gentner, B., Cantore, A., Colleoni, S., Amendola, M., Zingale, A., Baccarini, A., Lazzari, G., Galli, C., and Naldini, L. (2007). Endogenous microRNA can be broadly exploited to regulate transgene expression according to tissue, lineage and differentiation state. *Nat. Biotechnol.* 25, 1457–1467.
9. Miki, K., Endo, K., Takahashi, S., Funakoshi, S., Takei, I., Katayama, S., Toyoda, T., Kotaka, M., Takaki, T., Umeda, M., et al. (2015). Efficient detection and purification of cell populations using synthetic microRNA switches. *Cell Stem Cell* 16, 699–711.
10. Lagos-Quintana, M., Rauhut, R., Yalcin, A., Meyer, J., Lendeckel, W., and Tuschl, T. (2002). Identification of tissue-specific microRNAs from mouse. *Curr. Biol.* 12, 735–739.
11. Dong, H., Lei, J., Ding, L., Wen, Y., Ju, H., and Zhang, X. (2013). MicroRNA: function, detection, and bioanalysis. *Chem. Rev.* 113, 6207–6233.
12. Song, Y., Xu, Z., and Wang, F. (2020). Genetically encoded reporter genes for microRNA imaging in living cells and animals. *Mol. Ther. Nucleic Acids* 21, 555–567.
13. Kato, Y., Miyaki, S., Yokoyama, S., Omori, S., Inoue, A., Horiuchi, M., and Asahara, H. (2009). Real-time functional imaging for monitoring miR-133 during myogenic differentiation. *Int. J. Biochem. Cell Biol.* 41, 2225–2231.
14. Kato, Y., Sawata, S.Y., and Inoue, A. (2010). A lentiviral vector encoding two fluorescent proteins enables imaging of adenoviral infection via adenovirus-encoded miRNAs in single living cells. *J. Biochem.* 147, 63–71.
15. Sachdeva, R., Jönsson, M.E., Nelander, J., Kirkeby, A., Guibentif, C., Gentner, B., Naldini, L., Björklund, A., Parmar, M., and Jakobsson, J. (2010). Tracking differentiating neural progenitors in pluripotent cultures using microRNA-regulated lentiviral vectors. *Proc. Natl. Acad. Sci. USA* 107, 11602–11607.
16. Sano, M., Ohtaka, M., Iijima, M., Nakasu, A., Kato, Y., and Nakanishi, M. (2017). Sensitive and long-term monitoring of intracellular microRNAs using a non-integrating cytoplasmic RNA vector. *Sci. Rep.* 7, 12673.
17. Brown, B.D., Venneri, M.A., Zingale, A., Sergi, L., and Naldini, L. (2006). Endogenous microRNA regulation suppresses transgene expression in hematopoietic lineages and enables stable gene transfer. *Nat. Med.* 12, 585–591.
18. Åkerblom, M., Sachdeva, R., Quintino, L., Wettergren, E.E., Chapman, K.Z., Manfre, G., Lindvall, O., Lundberg, C., and Jakobsson, J. (2013). Visualization and genetic modification of resident brain microglia using lentiviral vectors regulated by microRNA-9. *Nat. Commun.* 4, 1770.
19. Chaudhury, A., Kongchan, N., Gengler, J.P., Mohanty, V., Christiansen, A.E., Fachini, J.M., Martin, J.F., and Neilson, J.R. (2014). A piggyBac-based reporter system for scalable *in vitro* and *in vivo* analysis of 3′ untranslated region-mediated gene regulation. *Nucleic Acids Res.* 42, e86.
20. Hong, S., Hwang, D.Y., Yoon, S., Isacson, O., Ramezani, A., Hawley, R.G., and Kim, K.S. (2007). Functional analysis of various promoters in lentiviral vectors at different stages of *in vitro* differentiation of mouse embryonic stem cells. *Mol. Ther.* 15, 1630–1639.
21. Norrman, K., Fischer, Y., Bonnamy, B., Wolfhagen Sand, F., Ravassard, P., and Semb, H. (2010). Quantitative comparison of constitutive promoters in human ES cells. *PLoS ONE* 5, e12413.
22. Amendola, M., Giustacchini, A., Gentner, B., and Naldini, L. (2013). A double-switch vector system positively regulates transgene expression by endogenous microRNA expression (miR-ON vector). *Mol. Ther.* 21, 934–946.
23. Ying, Z.M., Wu, Z., Tu, B., Tan, W., and Jiang, J.H. (2017). Genetically encoded fluorescent RNA sensor for ratiometric imaging of microRNA in living tumor cells. *J. Am. Chem. Soc.* 139, 9779–9782.
24. Lin, M.W., Tseng, Y.W., Shen, C.C., Hsu, M.N., Hwu, J.R., Chang, C.W., Yeh, C.J., Chou, M.Y., Wu, J.C., and Hu, Y.C. (2018). Synthetic switch-based baculovirus for transgene expression control and selective killing of hepatocellular carcinoma cells. *Nucleic Acids Res.* 46, e93.
25. Wang, X.W., Hu, L.F., Hao, J., Liao, L.Q., Chiu, Y.T., Shi, M., and Wang, Y. (2019). A microRNA-inducible CRISPR-Cas9 platform serves as a microRNA sensor and cell-type-specific genome regulation tool. *Nat. Cell Biol.* 21, 522–530.
26. Ezzine, S., Vassaux, G., Pitard, B., Barreau, B., Malinge, J.M., Midoux, P., Pichon, C., and Baril, P. (2013). RILES, a novel method for temporal analysis of the *in vivo* regulation of miRNA expression. *Nucleic Acids Res.* 41, e192.
27. Haurwitz, R.E., Jinek, M., Wiedenheft, B., Zhou, K., and Doudna, J.A. (2010). Sequence- and structure-specific RNA processing by a CRISPR endonuclease. *Science* 329, 1355–1358.
28. Horvath, P., and Barrangou, R. (2010). CRISPR/Cas, the immune system of bacteria and archaea. *Science* 327, 167–170.
29. Lee, H.Y., Haurwitz, R.E., Apffel, A., Zhou, K., Smart, B., Wenger, C.D., Laderman, S., Bruhn, L., and Doudna, J.A. (2013). RNA-protein analysis using a conditional CRISPR nuclease. *Proc. Natl. Acad. Sci. USA* 110, 5416–5421.
30. Qi, L., Haurwitz, R.E., Shao, W., Doudna, J.A., and Arkin, A.P. (2012). RNA processing enables predictable programming of gene expression. *Nat. Biotechnol.* 30, 1002–1006.
31. Nissim, L., Perli, S.D., Fridkin, A., Perez-Pinera, P., and Lu, T.K. (2014). Multiplexed and programmable regulation of gene networks with an integrated RNA and CRISPR/Cas toolkit in human cells. *Mol. Cell* 54, 698–710.
32. Tsai, S.Q., Wyvekens, N., Khayter, C., Foden, J.A., Thapar, V., Reyon, D., Goodwin, M.J., Aryee, M.J., and Joung, J.K. (2014). Dimeric CRISPR RNA-guided FokI nucleases for highly specific genome editing. *Nat. Biotechnol.* 32, 569–576.
33. Li, M., Husic, N., Lin, Y., Christensen, H., Malik, I., McIver, S., LaPash Daniels, C.M., Harris, D.A., Kotzbauer, P.T., Goldberg, M.P., and Snider, B.J. (2010). Optimal promoter usage for lentiviral vector-mediated transduction of cultured central nervous system cells. *J. Neurosci. Methods* 189, 56–64.
34. Borchardt, E.K., Vadoros, L.A., Huang, M., Lackey, P.E., Marzluff, W.F., and Asokan, A. (2015). Controlling mRNA stability and translation with the CRISPR endoribonuclease Csy4. *RNA* 21, 1921–1930.
35. Hoffmann, M.D., Aschenbrenner, S., Grosse, S., Rapti, K., Domenger, C., Fakhiri, J., Mastel, M., Börner, K., Eils, R., Grimm, D., and Niopek, D. (2019). Cell-specific CRISPR-Cas9 activation by microRNA-dependent expression of anti-CRISPR proteins. *Nucleic Acids Res.* 47, e75.
36. Suh, M.R., Lee, Y., Kim, J.Y., Kim, S.K., Moon, S.H., Lee, J.Y., Cha, K.Y., Chung, H.M., Yoon, H.S., Moon, S.Y., et al. (2004). Human embryonic stem cells express a unique set of microRNAs. *Dev. Biol.* 270, 488–498.
37. Bartel, D.P. (2018). Metazoan MicroRNAs. *Cell* 173, 20–51.
38. Bartel, D.P. (2009). MicroRNAs: target recognition and regulatory functions. *Cell* 136, 215–233.
39. Vidigal, J.A., and Ventura, A. (2012). Embryonic stem cell miRNAs and their roles in development and disease. *Semin. Cancer Biol.* 22, 428–436.
40. Wilson, K.D., Venkatasubrahmanyam, S., Jia, F., Sun, N., Butte, A.J., and Wu, J.C. (2009). MicroRNA profiling of human-induced pluripotent stem cells. *Stem Cells Dev.* 18, 749–758.
41. Valadi, H., Ekström, K., Bossios, A., Sjöstrand, M., Lee, J.J., and Lötval, J.O. (2007). Exosome-mediated transfer of mRNAs and microRNAs is a novel mechanism of genetic exchange between cells. *Nat. Cell Biol.* 9, 654–659.
42. Furuta, T., Miyaki, S., Ishitobi, H., Ogura, T., Kato, Y., Kamei, N., Miyado, K., Higashi, Y., and Ochi, M. (2016). Mesenchymal stem cell-derived exosomes promote fracture healing in a mouse model. *Stem Cells Transl. Med.* 5, 1620–1630.
43. Cui, Y., Wan, H., and Zhang, X. (2021). miRNA in food simultaneously controls animal viral disease and human tumorigenesis. *Mol. Ther. Nucleic Acids* 23, 995–1006.

44. Gismondi, A., Nanni, V., Monteleone, V., Colao, C., Di Marco, G., and Canini, A. (2021). Plant miR171 modulates mTOR pathway in HEK293 cells by targeting GNA12. *Mol. Biol. Rep.* 48, 435–449.
45. Aydemir, M.N., Aydemir, H.B., Korkmaz, E.M., Budak, M., Cekin, N., and Pinarbasi, E. (2021). Computationally predicted SARS-COV-2 encoded microRNAs target NFkB, JAK/STAT and TGFB signaling pathways. *Gene Rep.* 22, 101012.
46. Alamudi, S.H., and Chang, Y.T. (2018). Advances in the design of cell-permeable fluorescent probes for applications in live cell imaging. *Chem. Commun. (Camb.)* 54, 13641–13653.
47. Lienert, F., Lohmueller, J.J., Garg, A., and Silver, P.A. (2014). Synthetic biology in mammalian cells: next generation research tools and therapeutics. *Nat. Rev. Mol. Cell Biol.* 15, 95–107.
48. Hirotsawa, M., Fujita, Y., Parr, C.J.C., Hayashi, K., Kashida, S., Hotta, A., Woltjen, K., and Saito, H. (2017). Cell-type-specific genome editing with a microRNA-responsive CRISPR-Cas9 switch. *Nucleic Acids Res.* 45, e118.
49. Sano, M., Iijima, M., Ohtaka, M., and Nakanishi, M. (2016). Novel strategy to control transgene expression mediated by a Sendai virus-based vector using a nonstructural C protein and endogenous microRNAs. *PLoS ONE* 11, e0164720.
50. Wada, S., Kato, Y., Okutsu, M., Miyaki, S., Suzuki, K., Yan, Z., Schiaffino, S., Asahara, H., Ushida, T., and Akimoto, T. (2011). Translational suppression of atrophic regulators by microRNA-23a integrates resistance to skeletal muscle atrophy. *J. Biol. Chem.* 286, 38456–38465.